PROCEEDINGS OF THE 2ND NORTH AMERICAN ROCK MECHANICS SYMPOSIUM: NARMS'96
A REGIONAL CONFERENCE OF ISRM/MONTRÉAL/QUÉBEC/CANADA/ 19-21 JUNE 1996

Rock Mechanics Tools and Techniques

Edited by
MICHEL AUBERTIN
Ecole Polytechnique, Montréal, Québec, Canada
FERRI HASSANI
McGill University, Montréal, Québec, Canada
HANI MITRI
McGill University, Montréal, Québec, Canada

OFFPRINT

A.A. BALKEMA/ROTTERDAM/BROOKFIELD/1996

Rock Mechanics, Aubertin, Hassani & Mitri (eds) © 1996 Balkema, Rotterdam. ISBN 90 5410 838 X

Two-dimensional nonlinear finite element analysis of well damage due to reservoir compaction, well-to-well interactions, and localization on weak layers

L. Brun Hilbert, Jr – *University of California at Berkeley, Calif., USA*
Joanne T. Fredrich – *Sandia National Laboratories, Albuquerque, N.Mex., USA*
Mike S. Bruno – *Terralog Technologies USA, Inc., Arcadia, Calif., USA*
Greg L. Deitrick & Eric P.de Rouffignac – *Shell Exploration and Production Company, Houston, Tex., USA*

ABSTRACT: In this paper we present the results of a coupled nonlinear finite element geomechanics model for reservoir compaction and well-to-well interactions for the high-porosity, low strength diatomite reservoirs of the Belridge field near Bakersfield, California. We show that well damage and failures can occur under the action of two distinct mechanisms: shear deformations induced by pore compaction, and subsidence, and shear deformations due to well-to-well interactions during production or water injection. We show such casing damage or failure can be localized to weak layers that slide or slip under shear due to subsidence. The magnitude of shear displacements and surface subsidence agree with field observations.

1 INTRODUCTION

The subject of this paper is the effect of ground subsidence and pore compaction on the damage and failure of oil wells in the Belridge field in Southern California. It is well known that subsurface rock formations can compact under the reduction of pore pressure, that is when interstitial fluids are removed (Poland, J.F. and Davis, G.H., 1969, Geertsma, 1973). Under large loads or a significant reduction of pore pressure, rock grains can fracture or become crushed and undergo translations and rotations thus filling pore space, a mechanism referred to as "pore collapse" (see, Wong, et al., 1992 and Wong, et al., 1996).

Pore compaction is expressed at the surface of the earth as subsidence, or sinking of the ground. The magnitude of subsidence can be large, as much as 30 feet in the case of the San Joaquin Valley groundwater withdrawal (Poland, J.F. and Davis, G.H., 1969), 29 feet in the Wilmington oil fields in southern California (Mayuga and Allen, 1969) and at least 13 feet in Ekofisk in the North Sea and continuing to subside (Boade, et al., 1988).

The forces associated with pore compaction and subsidence can be large and on the scale of an oil field, say several thousand feet in width, length and depth, a steel casing string that is 7 inches in diameter offers little resistance. Damage to and complete failure of well tubulars in subsiding oil fields can take the form of S-shaped bending or "kinking" at the flanks of the subsiding region and bending can cause tensile failure of the threaded connections, while compression can result in helical buckling, cross-sectional buckling (i.e., bulging) and telescope type thread shear. If the shearing or bucking of the casing or tubing is severe enough, then downhole tools may be impassable through the buckled section and the well can not be worked over. If this is the case, local regulations may preclude further production and may require abandonment of the well.

In this paper we report the results of analysis of subsidence in the Belridge Field, located near Bakersfield, California. We constructed a two-dimensional plane strain finite element model of a slice of the field using a commercially available general-purpose finite element program (Hibbitt, et al., 1994). A geoemechanical model consisting of mixed displacement-pore pressure elements was coupled to a two-dimensional reservoir simulator to capture the constitutive behavior of the formation rocks during oil and gas production and water injection. To model failure of weak layers, such as weak shales, we used contact elements. In Section 2 of this paper we describe the relevant aspects of the Belridge field and the subsurface environment. In Section 3 we describe the coupled geomechanics-reservoir model and modeling procedures. In Section 4 we present results obtained to date (this project is ongoing and we expect to report on further developments in the near future). In Section 5 we discuss observations and conclusion made from a review of the modeling results.

2 PROBLEM DESCRIPTION

The Belridge field is located in Kern County California, which is west of Bakersfield, as shown in Figure 1. An idealized geologic cross section is shown in Figure 2. The diatomite and upper porcelanite formations are completed and produced together, but separately from the shallower Tulare sanstones. The Tulare sands have been subject to a steam flooding for several years, while some steam flooding pilots in the diatomite are underway currently.

Wellbore damage and failures associated with pore compaction and subsidence in the Belridge field have been documented in several previous papers.

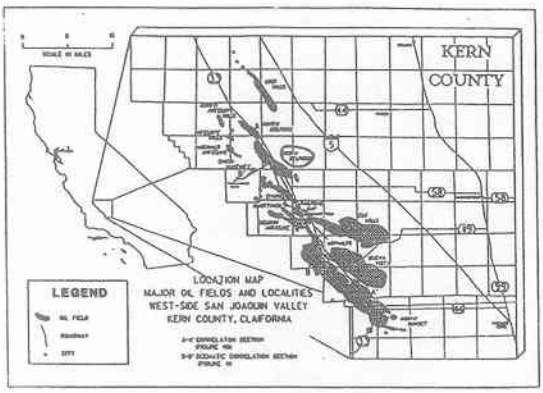

Figure 1. Belridge field and surrounding area.

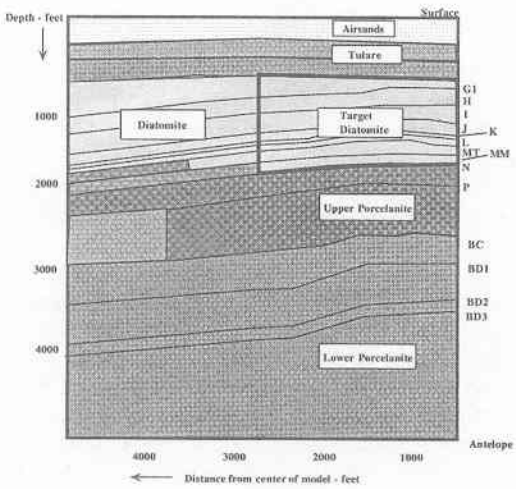

Figure 2. Idealized lithology and stratigraphy for Section 33 of the Belridge Field.

Bowersox and Shore (1990) described subsidence in Section 12 of the field, which included about 12.5 feet of surface subsidence and the appearance of surface fissures at the flanks of the subsiding region. They also provided well failure and damage statistics up through the end of 1987. Hansen, et al. (1993) and de Rouffignac, et al. (1995) presented results of two-dimensional finite element models of cross sections of the field. Hansen, et al. (1993) modeled the diatomite using an elasto-plastic constitutive law based on the Drucker-Prager model and included the thermal effects of steam flooding in the Tulare sands. Their model was successful in predicting the locations of surface fissures, the magnitude of subsidence, and was consistent with the mode of casing damage and failure mechanisms.

de Rouffignac, et al. (1995) incorporated an extended Drucker-Prager model for the diatomite that included a "cap" yield surface to capture plastic deformation resulting from pore collapse. Their results showed less elastic rebound at the surface under water injection than predicted by Hansen, et al. (1993) due to incorporation of the cap yield surface. Their results also indicated the potential for casing damage due to well-to-well interactions under production and water injection.

3 MODEL DESCRIPTION

3.1 *Model Geometry*

The two-dimensional model used in this study represents a planar slice of Section 33 of the South Belridge field. The location of the slice is depicted as a thick line in the plan view of Section 33 shown in Figure 3. It is assumed that the section is symmetric about the long axis of the field and based on field development this is appears to be a fair assumption. The particular slice was chosen also because it cuts through or is very near several wells, and thus there is some experience with the life of particular wells.

The finite element mesh is shown in Figure 4. The section outlined in thick lines is the area of the model in which incremental pore pressures were prescribed, which will be discussed later. It extended to a depth of 4800 feet and laterally to the left a distance of 3970.5 feet. The model had 6543 nodes and 1696 8-node reduced integration biquadratic displacement, bilinear pore pressure finite elements. The model included mechanical descriptions of 12 distinct layers of geomaterials, according to rock type.

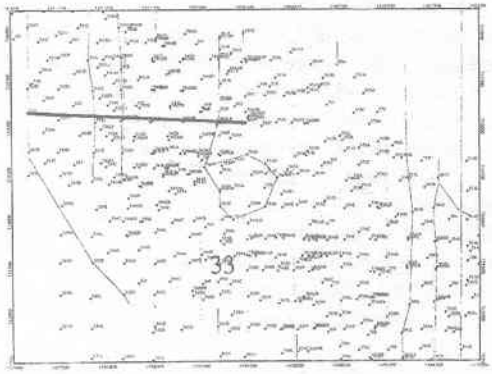

Figure 3. Plan view of Section 33 showing model location.

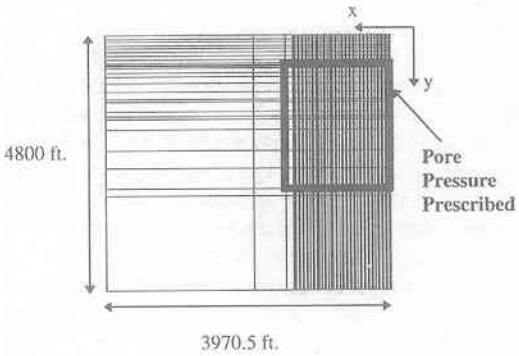

Figure 4. Finite element mesh for South Belridge Section 33 two-dimensional model.

Table 1. Layer thicknesses and material elastic properties.

Layer*	Thickness (ft)	Young's Modulus (psi)	Poisson Ratio	Density $\times 10^{-3}$ (lb/in^3)
Airsands	308.2	18,000	0.30	68.64
Up. Tulare	212.3	35,000	0.25	38.16
Lo. Tulare	95.3	35,000	0.25	38.16
Diatomite:				
G	158.2	47,700	0.17	19.51
H	121.5	63,000	0.17	19.51
I	159.3	79,200	0.19	19.51
J	152.0	60,000	0.20	19.51
K	43.2	71,600	0.17	19.51
L	186.8	112,400	0.17	19.51
M	129.0	162,600	0.17	19.51
Up. Porc.	587.0	68,000	0.22	28.54
Lo. Porc.	2647.0	360,000	0.29	33.96

*Up.=Upper, Lo.=Lower, Porc.=Porcelanite

Geologic layer thicknesses and elastic material properties are listed in Table 1 (material constitutive behavior is addressed below). The layer thicknesses are average values from the as-known stratigraphy of the cross section. The overburden and diatomite actually vary in thickness, but the results indicate that the model used herein produced results consistent with field observations. Future developments include a more detailed model with the curvature of the formations.

The boundary conditions on the finite element model are that nodes on the right and left side are constrained to move only vertically and the lower edge of the model is constrained to allow lateral motion only. Boundary effects from the left side of the model are minimal, as established in earlier work (see Hansen, et al., 1993 and de Rouffignac, et al., 1995).

3.2 *Constitutive Models*

Strickland (1985) characterized the diatomite rock as "principally amorphous opaline silica diatoms with only a trace of crystoballite quartz or chert quartz." It was observed that the diatomite can exhibit inelastic and plastic behavior due to pore collapse and can show creep behavior in the long term.

Constitutive models were developed through extensive tests on samples from cores and are based on additional tests to enlarge a data base of material properties reported previously (see Hansen, et al., 1993 and de Rouffignac, et al., 1995). The elastic properties were listed in Table 1. It can be observed that the density of the diatomite is significantly less than that of the other rock types. This is consistent with its high porosity, up to 55%, and low strength.

The airsands, Tulare sands, and Porcelanite rocks were modeled with a Drucker-Prager shear failure surface. The diatomite layers were modeled using a multi-surface yield criterion: a Drucker-Prager shear failure surface, a cap surface to capture plastic compaction (i.e., pore collapse), and a transition surface to join the two surfaces. The Drucker-Prager and transition surfaces use nonassociated flow rules and the cap surface uses an associated flow.

Some comments are in order regarding the constitutive models used in this study. First, it is known that diatomite is capable of creep and operators in this field indicate that some well damage may be a result of creep (Hansen, et al., 1993, and de Rouffignac, et al. 1995). Such time dependent deformation was not included in the current modeling work, but is the subject of ongoing research. Second, the development of computational constitutive models for rock is an area of active research. Some investigators have advocated using a curved shear failure envelope, rather than the linear Drucker-Prager surface (e.g., Wong, et la., 1996 and

DiMaggio and Sandler, 1971) or critical state Cam-Clay, end-cap surfaces (Schofield and Wroth, 1968). This too is an area for future research on diatomite modeling. Third, it is known that actual rocks exhibit considerable hysteresis during loading, unloading and reloading (see, e.g., Hilbert, et al., 1994, and de Rouffignac, et al., 1994). The actual effects of hysteresis and non-proportional loading are unclear and are expected to be complex (see, e.g, Wong, et al., 1992).

3.3 *Behavior of weak layers*

The depositional Tulare sands above the diatomite reservoir include thin layers of sandy-silts, mudstones, and clays (McPherson and Miller, 1994). The sands are produced by some operators in Belridge and are subjected to steam flooding. Several operators in the field have reported casing damage and failure at depths corresponding to the locations of shale or clay zones in the sands (see Bowersox and Shore, 1990, Hansen, et al., 1993 and de Rouffignac, et al., 1995). Moreover, the geometry of the casing shear damage or failures is in many cases localized to lengths of a only few feet, which is consistent with the thickness of the weak layers exhibited in wellbore logs. It has been suggested that steamflooding could weaken the layers, allowing slip or shear deformation.

Hamilton, et al. (1994) investigated subsidence and well damage in the Wilmington field, which has the same general lithology and stratigraphy as Belridge. The particular focus of their model was to incorporate shear failure of weak layers with subsequent relative sliding, or slip, between layers. The behavior of a failed weak layer was modeled as a sliding interface, which is the same approach implemented in the work reported in this paper. Shear displacements, or slip, reached as much as several inches to several feet in their analysis, depending on the amount of subsidence, and is in agreement with field observations and consistent with reported casing damage. They "calibrated" the frictional resistance, or friction angle, of the weak layer in the model by comparing the predicted subsidence with reported field measurements. While they tested models with friction angles ranging from 6° to 15°, their modeling showed that a friction angle of 10° provided the best agreement between predicted and observed subsidence.

In our work to date we have used a friction angle of about 6°. While this appears to be a low value for frictional resistance, it is consistent with the low end of observed values for shales rich in montmorillonite (Goodman, 1989). Moreover, it is to be expected that the effect of high temperatures due to steam flooding of the Tulare may reduce the frictional resistance of the shales (notwithstanding any increase in strength or embrittlement due to drying effects).

The interface elements used in the model were for interactions between 8-node coupled displacement-pore pressure elements, capable of infinitesimal sliding between the surfaces. Six layers of interface elements were placed within and between the Upper and Lower Tulare sands and also between the Lower Tulare and Diatomite formation.

3.4 *Coupled analysis procedures and loading history*

The finite element model was coupled to a reservoir simulator. We refer to this geomechanics model as "weakly" coupled in the following sense: there was no coupling between pore fluid flow and deformation of the porous media. The element technology is based on an effective porous continuum, although there were discrete sliding interfaces between layers. Under actual conditions, changing stresses will cause changes in pore volume and concomitant changes in permeability. Pore collapse will also result in more significant changes in rock flow properties.

Our procedure consisted of an incremental analysis of marching through a history of prescribed pressure fields. The procedure began with a geostatic step in which the initial vertical and horizontal subsurface stress state was established. This was followed by a sequence of sixteen load steps corresponding to sixteen years of field history, from 1977 to 1992. For each step, increments of pore pressure, computed using a finite difference reservoir simulator, were prescribed to nodes within the outlined section of the mesh in Figure 4. For each step, a Newton procedure was used to solve the equations of equilibrium, which were nonlinear because of the elasto-plastic constitutive laws for the porous medium and the kinematic formulation of the interface elements.

Pore pressure distributions for the finite element model are shown as contour plots for the years 1986, 1987, and 1992 in Figure 5. These time steps are important since they correspond to the end of primary production in 1986 and the beginning of a water injection program in 1987, which was initiated to mitigate the subsidence problem. It is to be noted that a history match of the pressures computed with the reservoir model was conducted.

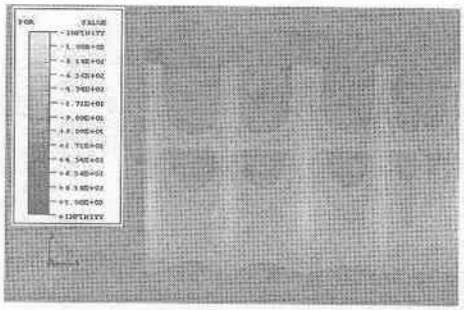

(a) 1986

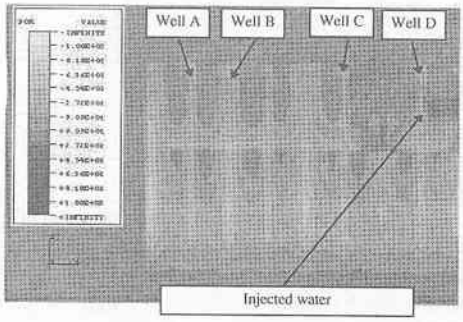

(b) 1987

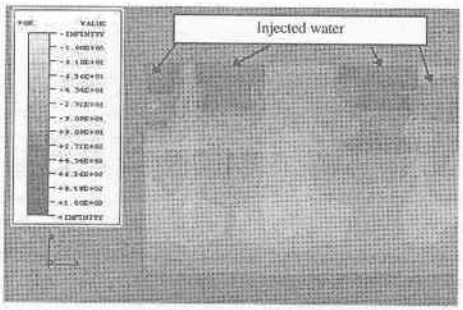

(c) 1992

Figure 5. Pore pressure distributions prescribed in finite element model as computed from reservoir simulator.

4 RESULTS

The geomechanics model was analyzed for two conditions: a "continuous" model in which a high friction angle (denoted as "infinite friction angle") was used to prohibit shear failure of the interfaces, and a model with a friction angle of 6°.

Curves of the nodal displacements on the surface of the model are shown in Figure 6. Both models predict essentially the same magnitude of subsidence, about 5 feet. This magnitude of subsidence is in agreement with field observations for Section 33. It is interesting that the sliding interface affects the subsidence expression on the flanks, however the changes are so slight that it is not practicable to measure this shape difference in the field as an attempt to determine if there are shearing weak layers.

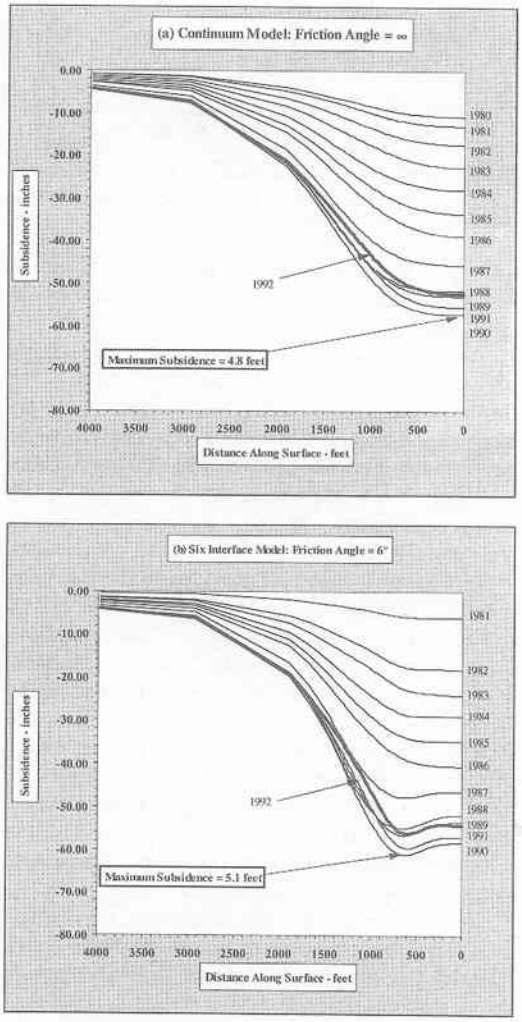

Figure 6. Curves of surface subsidence.

The maximum subsidence on a yearly basis and the rate of subsidence, both shown in Figure 7, are also consistent with field measurements. It can be observed that the subsidence rate is as high as 7-inches per year before the water injection program

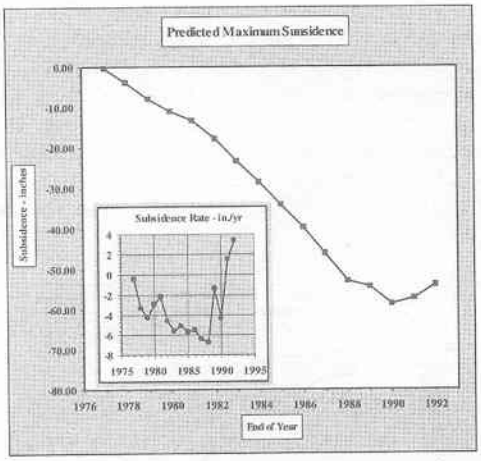

Figure 7. Predicted maximum subsidence and rate.

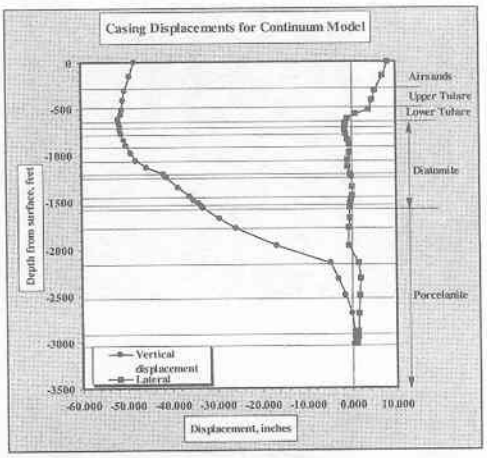

Figure 8. Casing deformations.

reverses the subsidence. The small amount of surface "rebound" during the last three years is in agreement with field observations.

To investigate the deformation of the casing under the prescribed loading history, the displacements of nodes lying in a vertical line at the location of a well have been plotted. Considering the fact that the diameter of the casing is from 5-inches to 7-inches, it is appropriate to assume that casing string will deform with the rock strata (of course, this does not address local casing-cement-rock interaction, or the support provided to the casing by the surrounding material, which is a matter of current research by other investigators). Four well locations are considered: Wells A and B, located on the flank of the subsiding region of the model and Wells C and D, located near the center of the model. The locations of these study wells are shown in Figure 5(b). Concentration is focused on the years 1986, 1987 and 1992 of the load history, which corresponds to the end of primary production, the initiation of the water injection program, and several years of the water injection program, respectively.

As an example to set conventions, the vertical and lateral displacements of one of the wells for an arbitrary year are plotted in Figure 8 (the plot is from the "continuum" model). Also plotted in this figure are the depths of the various rock strata. It can be seen that the vertical displacements are always negative, corresponding to pore compaction (plastic deformation) of the diatomite. The lateral displacements are much more complicated, and indicate the potential for large shear displacements at the interface between the Lower Tulare and diatomite rocks.

A plot of lateral displacements for wells A, B, C, and D for the model with six sliding interfaces is shown in Figure 9. Note that the scales for lateral displacement vary among plots. For wells A and B, located on the left flank of the model where the curvature of the deformed layers is greatest, it is observed that there are large magnitudes of lateral displacement at the Tulare-diatomite interface at about 600 feet. This is consistent with the depth and location of casing damage in the field. Wells C and D are located in what is typically assumed to be the "flat" portion of the subsidence region in the center of the field, where there is little, if any, curvature associated with subsidence. However, the wells are subjected to localized shear deformations at the Tulare-diatomite interface. These localized shear displacements are due to the deformations induced by the injection of water, as can be deduced from Figures 5(b) and (c). It can be seen in Figure 9 that wells C and D undergo large shear displacements at between 1986 and 1987. The shear displacements are exacerbated by the injection of greater volumes of water up to 1992.

Relative slip between the Tulare-diatomite interface are shown Figure 10. The slip magnitudes are not expressed as a smooth, symmetric curve, as is typically depicted for a subsidence "bowl". Rather, due to production of oil and gas and injection of water there are considerable effects as a result of well-to-well interaction. Even during oil production alone (i.e., 1986), shear slip can be up to 4 inches, which may be sufficient to cause permanent

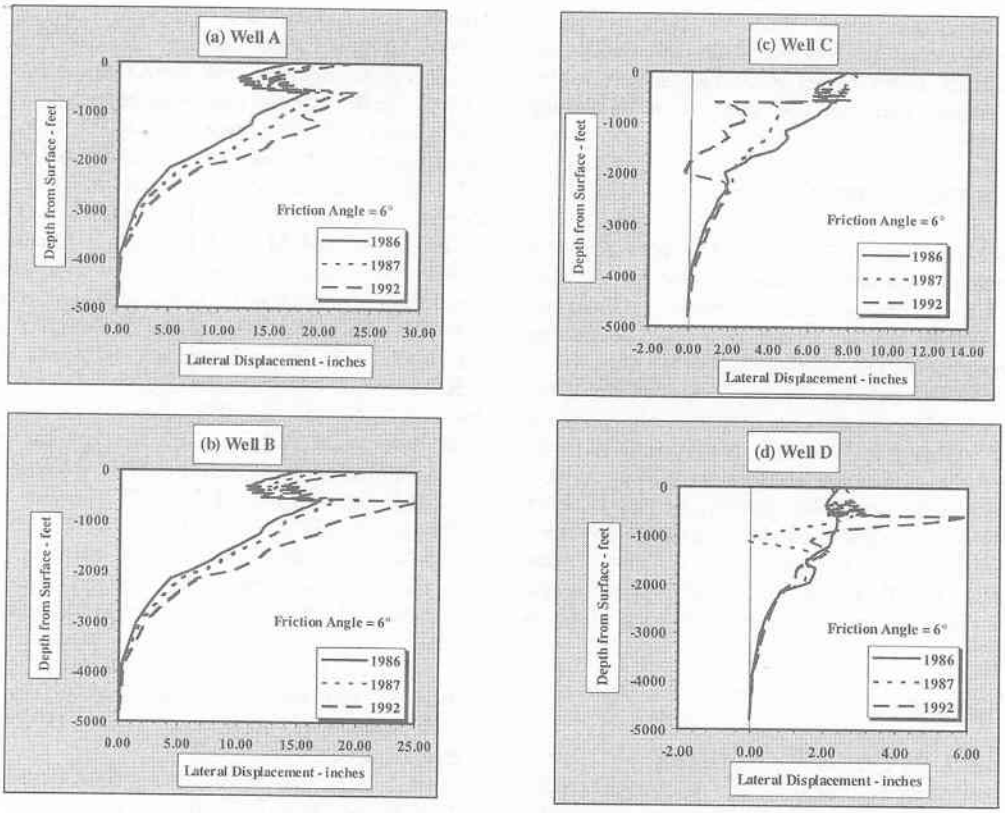

Figure 9. Lateral displacements of wells.

deformation and damage to the casing. This may explain the cases of well damage and failures observed by several of the operators in the field prior to the advent of water injection programs. It can be observed that by 1992 some areas of the field may experience up to a foot of slip due to well-to-well interactions.

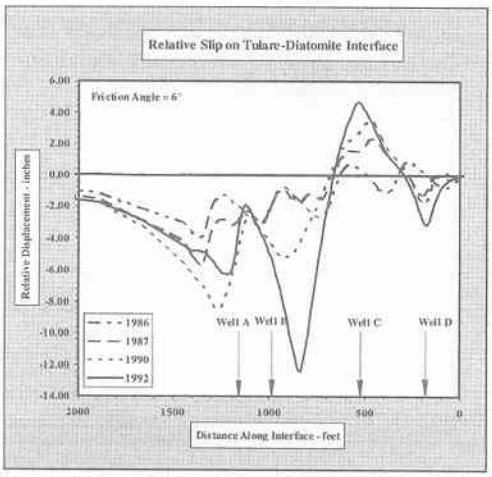

Figure 10. Relative slip along entire Tulare-diatomite interface.

5 CONCLUSIONS AND DISCUSSION

We have conducted a coupled reservoir flow-geomechanics analysis of a portion of the Belridge field to determine the origin and mechanisms of well damage. The analysis results show that well-to-well interactions during production as well as during water injection can cause sufficiently large shear deformations to cause well damage or even failure. Such well damage in the form of permanently deformed kinked or bent casing, compressive buckling, and tension failure under combined bending and shearing deformations and loads can explain many of the failure observed in the field.

Mitigation of damage and failures requires not only failure analysis based upon field observations and historical records, but also on a field program to monitor the geotechnical deformations, such as

subsidence monuments. Moreover, casings could be instrumented to observe downhole deformations, or logs, such as tilt meters could be run with a pre-determined frequency as part of a monitoring program.

6 ACKNOWLEDGMENTS

This work was performed at Lawrence Berkeley National Laboratory and was supported by the U.S. Dept. of Energy under contract DE-AC03-76SF00098 and at Sandia National Laboratories under contract DE-AC04-94AL85000. The authors wish to acknowledge the help and opinions of Dr. Larry R. Myer of Lawrence Berkeley Laboratory and Drs. Wolfgang R. Warwersik and Lupe G. Arguello of Sandia National Laboratory. The authors acknowledge permission from Lawrence Berkeley National Laboratory, Sandia National Laboratory, Cal Resources, Chevron, Crutcher Tufts, Exxon, Mobil, Sante Fe Energy, and Shell Exploration and Production Company for permission to publish this paper.

7 REFERENCES

Boade, R.R., Chin, L.Y., and Siemers, W.T., 1988. Forecasting of Ekofisk Reservoir Compaction and Subsidence by Numerical Simulation, *Proc. 1988 Offshore Tech. Conf.*, Paper OTC 5622.

Bowersox, J.R. and Shore, R.A, 1990. Reservoir compaction of the Belridge diatomite and surface subsidence, South Belridge field, Kern County, California, *Structure and Stratigraphy and Hydrocarbon Occurences of the San Joaquin Basin*, California, Kuespert, J.A. and Reid, S.A., eds., *Assoc. Pet. Geol.*, p. 225-230.

de Rouffignac, E., Karanikas, J.M., Bondor, P.L., Hara, S.K., 1995. Subsidence and Well Failure in the South Belridge Diatomite Field, , *SPE Proc. SPE Western Regional Mtg.*, SPE 29626, 1-15.

Di Maggio, F.L. and Sandler, I.S., 1971. Material model for granular soils, *J. Eng. Mech. Div., ASCE*, **97**:935-950.

Frame, R.G., 1952. Earthquake Damage, Its Cause and Prevention in the Wilmington Oil Field, Annual Report, Calif, Dept. Nat. Res., Div. Oil & Gas, San Francisco, CA, **38**:5-16.

Geertsma, J., 1973. Land subsidence above compacting oil and gas reservoirs, *J. Pet. Tech.*, **25**:734-744.

Goodman, R.E,. 1980. *Introduction to Rock Mechanics*, Wiley & Sons, New York, 2nd edition.

Hansen, K.S., Prats, M., and Chan, C.K., 1993. Finite-Element Modeling of Depltion-Induced Reservoir Compaction and Surface Subsidence in the South Belridge Oil Field, California, *SPE Proc. SPE Western Regional Mtg.*, SPE 26074, 437-452.

Hibbitt, Karlsson & Sorensen, Inc., 1994. ABAQUS Theory Manual, version 5.4, Pawtucket, RI.

Hilbert, L.B., Jr., Hwong, T.K., Cook, N.G.W., Nihei, K.T., and Myer, L.R., 1994. Effects of strain amplitude on the static and dynamic nonlinear deformation of Berea sandstone, *Proc. First N. Amer. Rock Mech. Symp.*, Nelson, P.P and Laubach, S.E., eds., Rotterdam, Balkema, 497-504.

Mayuga, M.N and Allen, D.R., 1969. Subsidence in the Wilmington Oil Field, Long Beach, California, U.S.A., *Proc. Tokyo Symp.: Int.Asso. Sci. Hydrol.*, IASH-Unesco-WMO, vol. 1, 66-79.

McPherson, J.G. and Miller, D.D., 1994. Depositional settings and reservoir characteristics of the plio-pleistocene Tulare formation, South Belridge field, San Joaquin Valley, California, in *Structure, Stratigraphy, and Hydrocarbon Occurances of the San Joaquin Basin*, 205-214.

Poland, J.F. and Davis, G.H., 1969. Land subsidence fluid withdrawal, *Rev. Eng. Geol.*, **II**, GSA, Boulder, CO.

Schoflied, A.N. and Wroth, C.P., 1968. *Critical State Soil Mechanics*, McGraw Hill, London.

Wong, T.-F., Szeto, H., and Zhang, J., 1992. Effecto of Loading Path and Porosity on the Failure Model of Poous Rocks, in *Micromechanical modelling of quasi-brittle materials behavior*, Li, V.C., ed., Appl. Mech., **45**:281-293.

Wong, T.-F., David, C., and Zhu, W., 1996. The transition from brittle faulting top cataclastic flow in porous sandstones: Mechanical Deformation, submitted to *J. Geophys. Res.*